Environ Sci Pollut Res (2016) 23:19134–19144
DOI 10.1007/s11356-016-7054-x

RESEARCH ARTICLE

Elimination of radiocontrast agent diatrizoic acid by photo-Fenton process and enhanced treatment by coupling with electro-Fenton process

Elvira Bocos[1,2] · **Nihal Oturan**[2] · **Marta Pazos**[1] · **M. Ángeles Sanromán**[1] · **Mehmet A. Oturan**[2]

Received: 6 May 2016 / Accepted: 7 June 2016 / Published online: 28 June 2016

Abstract The removal of radiocontrast agent diatrizoic acid (DIA) from water was performed using photo-Fenton (PF) process. First, the effect of H_2O_2 dosage on mineralization efficiency was determined using ultraviolet (UV) irradiation. The system reached a maximum mineralization degree of 60 % total organic carbon (TOC) removal at 4 h with 20 mM initial H_2O_2 concentration while further concentration values led to a decrease in TOC abatement efficiency. Then, the effect of different concentrations of Fenton's reagents was studied for homogeneous Fenton process. Obtained results revealed that 0.25 mM Fe^{3+} and 20 mM H_2O_2 were the best conditions, achieving 80 % TOC removal efficiency at 4 h treatment. Furthermore, heterogeneous PF treatment was developed using iron-activated carbon as catalyst. It was demonstrated that this catalyst is a promising option, reaching 67 % of TOC removal within 4 h treatment without formation of iron leachate in the medium. In addition, two strategies of enhancement for process efficiency are proposed: coupling of PF with electro-Fenton (EF) process in two ways: photoelectro-Fenton (PEF) or PF followed by EF (PF-EF) treatments, achieving in both cases the complete mineralization of DIA solution within only 2 h. Finally, the Microtox tests revealed the formation of more toxic compounds than the initial DIA during PF process, while, it was possible to reach total mineralization by both proposed alternatives (PEF or PF-EF) and thus to remove the toxicity of DIA solution.

Keywords Diatrizoic acid · Photo-Fenton · Mineralization · Heterogeneous process · Activated carbon · Photoelectro-Fenton

Responsible editor: Vítor Pais Vilar

Highlights
- Optimization of key parameters in photo-Fenton (PF) removal of diatrizoic acid (DIA)
- Eighty per cent TOC removal under homogeneous PF using 0.25 mM Fe^{3+} and 20 mM H_2O_2
- Sixty-seven per cent TOC removal under heterogeneous PF using iron-activated carbon
- Complete mineralization by photoelectro-Fenton (PEF) or PF followed by EF process (PF-EF)
- Removal of the toxicity of DIA solution by PEF or PF-EF

✉ Mehmet A. Oturan
mehmet.oturan@univ-paris-est.fr

[1] Department of Chemical Engineering, University of Vigo, Isaac Newton Building, Campus As Lagoas Marcosende, 36310 Vigo, Spain

[2] Laboratoire Géomatériaux et Environnement (LGE), Université Paris-Est, EA 4508, 77454 Marne-la-Vallée, France

Introduction

Over the past decades, pharmaceuticals have become problematic pollutants in both surface and groundwater. The presence of these pollutants in water streams is overall caused by pharmaceutical industrial streams, hospital waste and municipal wastewater effluents. Although they have been present in water from many years ago, the pollution of water has been highlighted in the 1960s when the presence of these compounds on the environment was detected in the USA and Europe (Stumm-Zollinger and Fair 1965). Usually, pharmaceuticals are found in very low quantities (ng L^{-1} to μg L^{-1}), and their behaviour in biotic and abiotic environments is still unknown (Daughton and Ternes 1999). Recently, some studies have demonstrated their potential hazards (Rastogi et al. 2014; Tiehm et al. 2011) even at low concentrations, and thus concerns about their potential risk became worrying. Therefore, the problem of their elimination has arisen. To protect the environment from adverse effects of such pollutants, it is important

to treat wastewaters containing pharmaceutical residues using safe and effective methods before their discharge into natural water streams.

To date, conventional wastewater treatment plants have been designed to reduce parameters like BOD_5, COD or total suspended solids. Nonetheless, these plants are unable to eliminate the wide variety of persistent organic pollutants (POPs), such as pharmaceuticals, which are recalcitrant to biological degradation (Malato 2008; Murgolo et al. 2015). Therefore, pharmaceutical and personal care products pass generally through the conventional wastewater treatment plants without significant changes, entering into natural water system.

Radiopaque solutions are daily dosed in high amounts in hospitals for radiologic diagnostics and finally excreted since they are not completely metabolized. Among them, the diatrizoic acid (DIA) has been used as radiologic contrast agent since 1950. This compound can be oxidized in the nature by biotic or abiotic process resulting in by-products with more hazardous potential than the original molecule (Gur-Reznik et al. 2011; Laurencé et al. 2014). Besides, even when traditional chemical oxidants react with these drugs, they are unable to mineralize them since their oxidation stopped at the level of formation of more persistent intermediates (Real et al. 2009). The low removal of some recalcitrant compounds by conventional processes necessitates developing alternative technologies able to overcome the complete degradation of these pollutants in water.

Lately, advanced oxidation processes (AOPs) have emerged as a potential alternative able to afford the elimination of POPs and have been usually combined with other pretreatments (Dias et al. 2014; Moreira et al. 2014; Oturan and Aaron 2014; Zhao et al. 2014) in order to reduce operational cost and increase the efficiency of the treatment. These processes are based on the generation of a strong oxidant, mainly hydroxyl radicals ($^{\cdot}OH$), the second most powerful oxidant ($E°$ = 2.8 V/SHE) after fluorine (Krzeminska et al. 2015). The high reactivity and non-selectivity of these radicals lead to the oxidative degradation of POPs until complete mineralization (Pignatello et al. 2006; Brillas et al. 2009; Brillas 2014a; Moreira et al. 2013; Oturan and Aaron 2014)). Thus, the elimination of non-ionic iodinated contrast media from water has already been studied by different AOPs (Papoutsakis et al. 2015; Radjenovic et al. 2013; Velo-Gala et al. 2012). Real et al. (2009) studied the removal of diatrizoate in ultrapure water by different oxidation systems such as ozone, ultraviolet (UV) radiation or Fenton's reagent, finding the most satisfactory results by the use of UV-irradiated Fenton's reagent, reaching 64.7 % of degradation after 5 min of treatment. Similarly, Ternes et al. (2003) reported that DIA has showed high resistance to ozonation treatments, even combined with UV light, obtaining only 35 % mineralization. Recently, Murgolo et al. (2015) enhanced photocatalytic degradation of different pollutants such as diatrizoate, under artificial and solar-simulated light by the use of a new photocatalyst based on nano-sized TiO_2.

The photo-Fenton (PF) process has demonstrated to have greatly improved the oxidation efficiency of the classical Fenton's method. Thus, in this process, the classical Fenton's reaction (Eq. 1) takes place; however, the generation of $^{\cdot}OH$ could be increased by application of UV irradiation and using as catalyst soluble Fe^{3+} salt at pH around 3. At this pH, the predominant species of iron(III) is $Fe(OH)^{2+}$ (Eq. (2)) which strongly absorbs UV light and generates, according to Eq. (3), $^{\cdot}OH$ and ferrous ion which can react with H_2O_2 following Eq. (1) to form $^{\cdot}OH$. This concomitant generation of a great amount of $^{\cdot}OH$ accelerates strongly the oxidation rate of organic pollutants present in the solution (Bouafia-Chergui et al. 2010; Bouafia-Chergui et al. 2012; Diagne et al. 2009). As a consequence, UV irradiation of the solution brings two main advantages: (i) production of $^{\cdot}OH$ by photo-reduction of iron(III) and (ii) catalysis of the Fenton's reaction (Eq. 1) through regeneration of ferrous (Fe^{2+}) iron which acts as a catalyst.

$$Fe^{2+} + H_2O_2 \rightarrow Fe^{3+} + OH^- + {}^{\cdot}OH \quad (1)$$

$$Fe^{3+} + H_2O \rightarrow Fe(OH)^{2+} + H^+ \quad (2)$$

$$Fe(OH)^{2+} + h\upsilon \rightarrow Fe^{2+} + {}^{\cdot}OH \quad (3)$$

Recently, several studies have been focused on the improvement of the Fenton process by using heterogeneous iron catalysts, in order to avoid the generation of iron sludge, facilitating their reuse in continuous processes and avoiding their loss on the outflow (Daud and Hameed 2010; Iglesias et al. 2013; Russo et al. 2014). For that purpose, several organic matrixes, such as hydrogels of polyacrylamide or alginate, have been demonstrated to have good performance as heterogeneous catalysts in electro-Fenton (EF) process (Rosales et al. 2012; Barreca et al. 2014; Bocos et al. 2014; Fernández de Dios et al. 2015; Iglesias et al. 2015). Some authors have pointed out activated carbon (AC) as a promising inorganic matrix and rough alternative for metal fixation, given its high stability, high surface area and great adsorption capacity (Foo and Hameed 2009; Iglesias et al. 2015). Moreover, AC has been demonstrated to be itself a good catalyst due to its surface chemistry (Stüber et al. 2005). For instance, an interesting study using iron-loaded AC as heterogeneous catalyst during EF treatment has recently been accomplished by Iglesias et al. (2015). These authors demonstrated the suitability and efficiency of this catalyst on the decolourization and mineralization of a complex effluent such as a highly polluted winery wastewater. Furthermore, the study of the main reactions taking place on the process proved the increase on the generation of $^{\cdot}OH$ owing to the use of AC, hence confirming the catalytic properties of this material itself.

Based on the aforementioned considerations, in this study, the optimization of the key parameters (H_2O_2 and iron concentration) in the homogeneous PF process was carried out for the elimination of DIA from water. Besides, different catalysts such as iron sepiolite alginate beads and iron-activated carbon were developed, and the efficiency of this process was compared with homogeneous PF process. In the last stage, to achieve the complete mineralization, the PF process is coupled to the EF process. Two alternative treatments were evaluated: PF as pre-treatment for EF process (PF-EF) or irradiation of Fenton's reagent generated in an electrochemical cell by EF process (PEF). Furthermore, Microtox tests have been performed in order to determine the initial and final toxicity of all the treated solutions.

Materials and methods

Chemicals

The pharmaceutical DIA ($C_{11}H_9I_3N_2O_4$, also known as amidotrizoic acid, or 3,5-diacetamido-2,4,6-triiodobenzoic acid) was provided by Alpha Aesar. Reagent-grade sulphuric acid (98 %) and iron(III) sulfatepentahydrate ($Fe_2(SO_4)_3 \cdot 5H_2O$) were purchased from Acros Organics in analytical grade. Hydrogen peroxide (30 wt.%) was provided by Merck.

DIA solutions of concentration of 0.1 mM were prepared with ultrapure water obtained from a Millipore Milli-Q Simplicity 185 system with resistivity of >18 MΩ cm at 25 °C. The pH of solutions was adjusted to a desired value using analytical-grade sulphuric acid or sodium hydroxide (Acros).

Preparation of the heterogeneous catalysts

Iron sepiolite (FeS) and iron-activated carbon (Fe-AC) were prepared by adsorption processes following the protocols previously reported by Iglesias et al. (2013, 2015). For that, AC (granulated no. 2 QP provided by Panreac (Spain)) and sepiolite clay (provided by Tolsa S.A.) were immersed in iron-enriched solutions (using $Fe_2(SO_4)_3 \cdot 5H_2O$ as source of Fe^{3+} ions) and kept in agitation using a mechanical shaking agitator (Thermo Forma) at 150 rpm at 20 °C. Samples were taken periodically, and the solid was separated by centrifugation (Sigma 3K-18) for 15 min at 7000 rpm. The unadsorbed iron in the supernatant was determined with atomic absorption spectroscopy (Agilent 240FS). The iron uptake concentration was determined by the difference between the initial concentration and that found in the supernatant solution after the assay. All the adsorption studies were repeated three times; the reported value is the average of the measurements.

After the fixation of iron to sepiolite, iron sepiolite alginate beads (FeS-AB) were prepared by mixing 20 mL of a 1.5 % (*w*/*v*) sodium alginate aqueous solution (Iglesias et al. 2014; Rosales et al. 2012) with 1.6 g of iron sepiolite. The resulting slurry was stirred at 35 °C of temperature during 4 h and then added drop wise into a stirred solution of 0.1 M $CaCl_2$. The beads were then recollected and washed and stored in distilled water at 4 °C.

Photoreactor and experimental procedures

The experiments were performed in a batch photoreactor with a cylindrical 1.2 L borosilicate double-walled reaction vessel as shown in Fig. 1. The solution was continuously recirculated at a flow rate of 9.5 L min^{-1} by a peristaltic pump. A low-pressure mercury lamp (Heraeus Noblelight-NNI 40/20, 35 W) emitting at 253.7 nm was placed in a quartz tube vertically positioned in the middle of the photoreactor. The temperature of the solution was kept at 20 °C throughout all the assays.

In all the experiments, the pH value of the solution was adjusted to 3. In homogenous process, a given weight of iron salt was added and mixed with the initial untreated solution before the addition of H_2O_2. In heterogeneous process, different amounts of catalyst FeS-AB or Fe-AC were added. These catalysts were maintained in suspension by continuous recirculation of the bulk media. The time at which the UV lamp was turned on was considered time zero. Samples were taken periodically at different time intervals. They were centrifuged at 10,000 rpm for 5 min, and the supernatant was separated to be analysed for pH, DIA concentration and mineralization degree.

After heterogeneous treatment, the amount of iron present in the treated solution was determined spectrophotometrically by atomic absorption spectrometry (Agilent 240FS).

Characterization of Fe-AC

Scanning electron microscopy (SEM) images were obtained using a JEOL JSM-6700F equipped with an energy-dispersive spectrometric (EDS) Oxford Inca Energy 300 SEM and an accelerating voltage of 15 kV (Electron Microscopy Service, C.A.C.T.I, University of Vigo). AC with and without iron were coated with C for the SEM observation. These images were used to study the AC itself and the Fe-AC.

Electrochemical cell

In addition, two strategies of coupling PF with EF process have been proposed: (i) PF-EF, where PF was firstly applied (during 30 min) to the DIA solution and then this solution was subjected to EF (during 90 min) and (ii) PEF treatment, where the electrochemical cell in which Fenton's reagent is generated by EF process was irradiated by UV-C light. These experiments were carried out in a cylindrical electrochemical cell

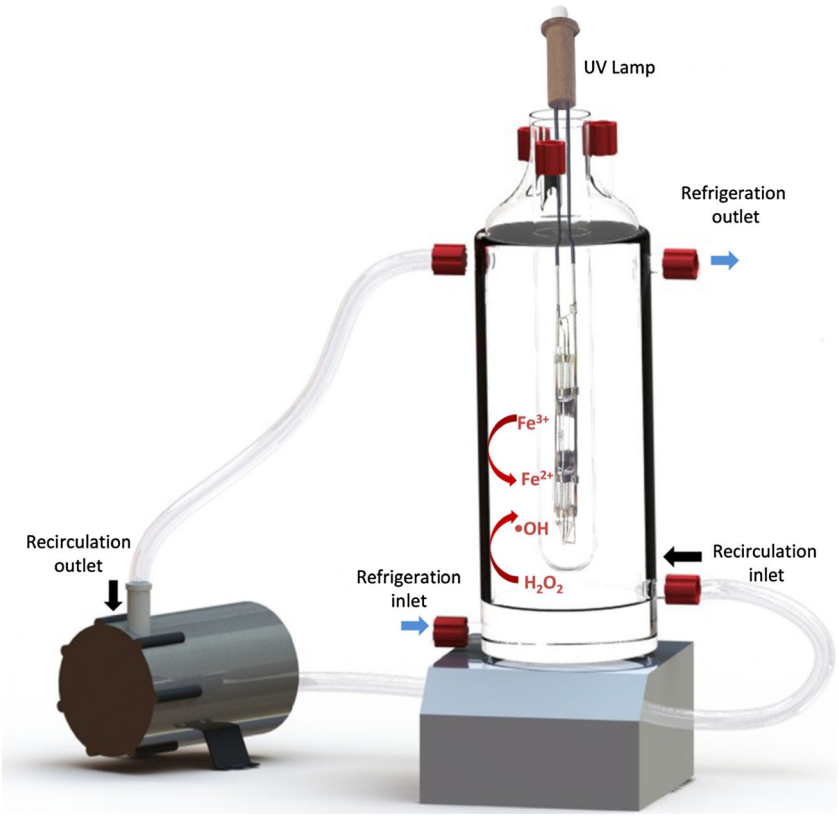

Fig. 1 Schematic presentation of the display used in this study for photo-Fenton process

refrigerated at 20 °C by a double jacket. In all cases, a suitable concentration of iron Fe^{3+} was added into the reactor as catalyst and the pH of the solution was kept at 3. Furthermore, in the photo-assisted experiments 20 mM of H_2O_2 were added into the bulk at the beginning of the assays. In the electrochemical assays, Carbon Felt (18 × 5 × 0.5 cm) and boron-doped diamond (BDD; 25 cm^2) were used as cathode and anode, respectively, applying a current intensity of 1 A, which has recently been reported by Bocos et al. (2016) as the optimum value in the degradation of DIA by EF process. Carbon felt was placed in the inner wall of the cell covering the total perimeter of the cell while BDD (3 × 3 cm) was centred in the reactor. Besides, the H_2O_2 was in situ electrochemically generated through the continuous aeration (1 L min^{-1}) on the cathode surface.

Analytical measurements

The pH of the solutions was measured using Eutech instruments digital pH metre. Total organic carbon (TOC) was measured before starting the treatment and after different treatment times in order to follow the mineralization degree of initial and treated samples with a Shimadzu VCSH TOC analyser. The calibration was performed using potassium hydrogen phthalate solutions as standard. Reproducible TOC values with an accuracy of ±1 % were found by injecting 50-μL aliquots into the analyser. The determination of concentration decay of DIA was monitored by high-performance liquid chromatography (HPLC) in the conditions previously optimized by Bocos et al. (2016).

Toxicity test

The potential toxicity of the initial sample of DIA and the global solution toxicity after the performed treatments were evaluated by using the bioluminescence of the marine bacteria *Vibrio fischeri* (Lumistox LCK 487), by means of the Microtox® method according to the international standard process. The inhibition ratio based on the test results was calculated using the following equation:

$$I = \left(1 - \left(L_S / L_C\right)\right) \times 100 \quad (4)$$

where I is the inhibition ratio (%) and L_S and L_C are the luminescence level of sample and control, respectively, after 15 min of exposition (Oh et al. 2015).

GC/MS analysis

Two hundred millilitres of the aqueous sample were extracted three times with 30 mL of ethyl acetate each time. After extraction, samples were dried with a rotary evaporator and

taken up to 200 μL of ethyl acetate that were analysed by gas chromatography mass spectrometry (GC/MS). Thus, the identification of the degradation products formed during the EF treatment was carried out by GC/MS analysis using a 6850 Agilent GC equipped with a 5955C VLMSD and a HP-5-MS column. Hydrogen was the carrier gas at a flow rate of 1.2 mL min^{-1}. For the GC separation, the GC injection port temperature was set at 280 °C. The programme temperature started at 50 °C (held during 5 min). Subsequently, the temperature ramp was set at 5 °C min^{-1} to 280 °C. The temperature was maintained at 280 °C for 5 min. The MS detector was operated in EI mode (70 eV).

Results and discussion

The concentrations of H_2O_2 and iron constitute the two main parameters in Fenton and related processes, thus the concentration ratio between them has special importance in terms of the removal of the pollutants and overall cost (Umar et al. 2010). Excess or scarcity of one of these reagents can promote parasitic reactions, reducing the efficiency of the process (Chiou et al. 2006; Bouafia-Chergui et al. 2010). Based on the above mentioned, it is necessary to improve the performance of the process throughout the optimization of the operating conditions.

Effect of H_2O_2 concentration on H_2O_2/UV-C photolysis efficiency

As it is well known, the photolysis of H_2O_2, as a consequence of UV-C light, produces an additional amount of $^{\cdot}OH$ according to Eq. (5), contributing to the degradation of organic pollutants. In order to optimize the operational conditions, the direct photolysis of 0.1 mM DIA solution was performed in presence of different molar concentrations of H_2O_2. Initially, the effect of UV-C light alone on the mineralization yields was evaluated. Unfortunately, it was not possible to follow the elimination of the parent compound by HPLC analysis, given its fast disappearance from the reaction media under the influence of UV-C light, as Velo-Gala et al. (2014) already pointed out in a study where the degradation of DIA was achieved in 1 min. Thus, the elimination of DIA was followed by means of the TOC decay.

$$H_2O_2 + h\upsilon \rightarrow 2(^{\cdot}OH) \quad (5)$$

Given the strong influence of the pH in the generation of $^{\cdot}OH$ and thus on the PF process efficiency, the solution pH was set around 3, because it exhibits the maximum catalytic activity (Pignatello and Sun 1995; Brillas et al. 2009). In addition, the pH of the solution remained almost constant along the treatment with a slight drop to a final value of 2.7–2.8 probably due to the generation of short-chain carboxylic acids (Florenza et al. 2015; García-Segura and Brillas 2011).

The insights of Fig. 2 show the evolution of TOC as a function of initial H_2O_2 concentration. It reveals that operating under constant intensity irradiance, the initial concentration of H_2O_2 is a critical variable on the oxidation of DIA. Although the mineralization rate under UV-C light irradiation was near 35 %; its enhancement by increasing H_2O_2 dosage is remarkable (Sirés and Brillas 2012; Hammouda et al. 2015) due to the formation of higher amount of $^{\cdot}OH$ according to Eq. (5). Mineralization rate increases when raising the concentration of H_2O_2 from 5 to 40 mM; whereas, further augmentations do not allow better mineralization efficiency. Despite that the pollutant degradation usually increases with the H_2O_2 dosage, an excessive addition does not improve the efficiency of the treatment owing to the decomposition of this reagent forming O_2 and H_2O (Neyens and Baeyens 2003). Moreover, this fact could be explained by an excess of H_2O_2 that promotes the scavenging of $^{\cdot}OH$ (Eq. 6), reducing the mineralization efficiency of the process (Rubio-Clemente et al. 2013; Loaiza-Ambuludi et al. 2014).

$$H_2O_2 + {}^{\cdot}OH \rightarrow H_2O + HO_2^{\cdot} \quad (6)$$

As can be deduced from Fig. 2, the mineralization efficiency of the pollutant was decreased for the concentrations of H_2O_2 higher than 40 mM. On the other hand, the maximum mineralization rate is close to that of 20 mM H_2O_2 dosage. Similarly, Ghaly et al. (2001) found that 20 mM was the optimum dosage for the photodegradation of the *p*-chlorophenol. Thus, it is shown that the efficiency of H_2O_2/UV-C photolysis can be improved by optimizing the concentration of H_2O_2, as previously reported by other authors (Ghaly et al. 2001; Barreca et al. 2014).

Effect of Fe^{3+} concentration in homogeneous PF process

One of the main parameters influencing the PF process is the concentration of iron ion used as catalyst. Recently, several reports (Bouafia-Chergui et al. 2010; Xu et al. 2015) have highlighted that high iron concentrations can decrease mineralization efficiency by promotion of the wasting reaction according to Eq. (7) which consumes $^{\cdot}OH$:

$$Fe^{2+} + {}^{\cdot}OH \rightarrow Fe^{3+} + OH^{-} \quad (7)$$

On the frame of this context, the effect of ferric iron concentration on TOC abatement was studied for the following values: 0.1, 0.25 and 0.5 mM. Additionally, these concentrations were tested with different amounts of H_2O_2 (5, 10 and 20 mM) in order to optimize the operational conditions.

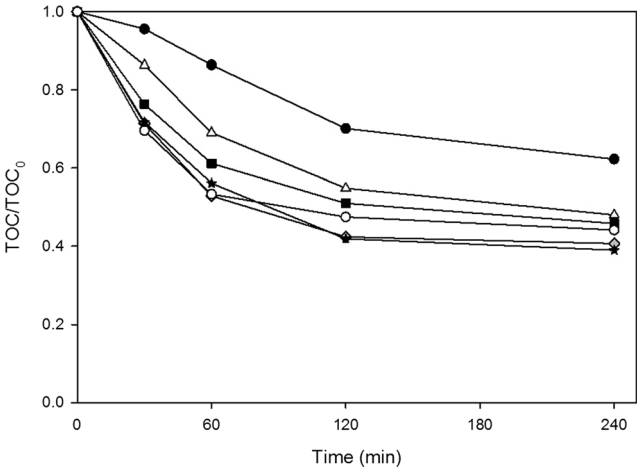

Fig. 2 Effect of the initial H_2O_2 dosage during the direct photolysis of 1.2 L of 0.1 mM DIA solutions at pH 3 as a function of the treatment time. H_2O_2 dosage, 0 mM (*black circle*), 5 mM (*white triangle*), 10 mM (*black square*), 20 mM (*grey square*), 40 mM (*black star*) and 100 mM (*white circles*)

As it can be seen on Fig. 3, the initial concentration of iron plays an important role in the TOC abatements during the PF treatment. Mineralization of 0.1 mM DIA solution was followed during 480 min; however, the data after 240 min are not shown on the figures since TOC removal values remained almost stable after this treatment times. Besides, as previously reported by Florenza et al. (2016), no significant variation of the pH (near 3.0) was found during all these trials. The evaluation of the results shown in Fig. 3 allows to conclude that TOC abatements were higher, for all H_2O_2 concentration, when the concentration of Fe^{3+} is increased from 0.1 to 0.25 mM, reaching the maximum value of 80 % TOC removal after 240 min for 20 mM H_2O_2 dosage. Nevertheless, when this concentration was increased until 0.5 mM, a decrease on the TOC abatement was detected, obtaining even lower values than that obtained for 0.1 mM catalyst concentration. This fact can be explained by the enhancement of the scavenging reaction promoted by the excess of Fe^{3+} (Eq. 7) (Rubio-Clemente et al. 2015).

Taking into account the obtained results for H_2O_2 photolysis (Fig. 2) and the data depicted in Fig. 3, the concentrations of 20 mM H_2O_2 and 2.5 mM Fe^{3+} seem to be the most adequate quantities of Fenton's reagent, allowing 80 % TOC removal after 4 h of treatment. In addition, the analysis of pH at the end of the treatment revealed a slight acidification (from 3 to 2.7). This fact was attributed to the possible formation of short-chain carboxylic acids generated along the treatment (Bocos et al. 2016).

Heterogeneous PF process

As it has been mentioned in the "Introduction", during the last years, iron(III) has been fixed in a wide variety

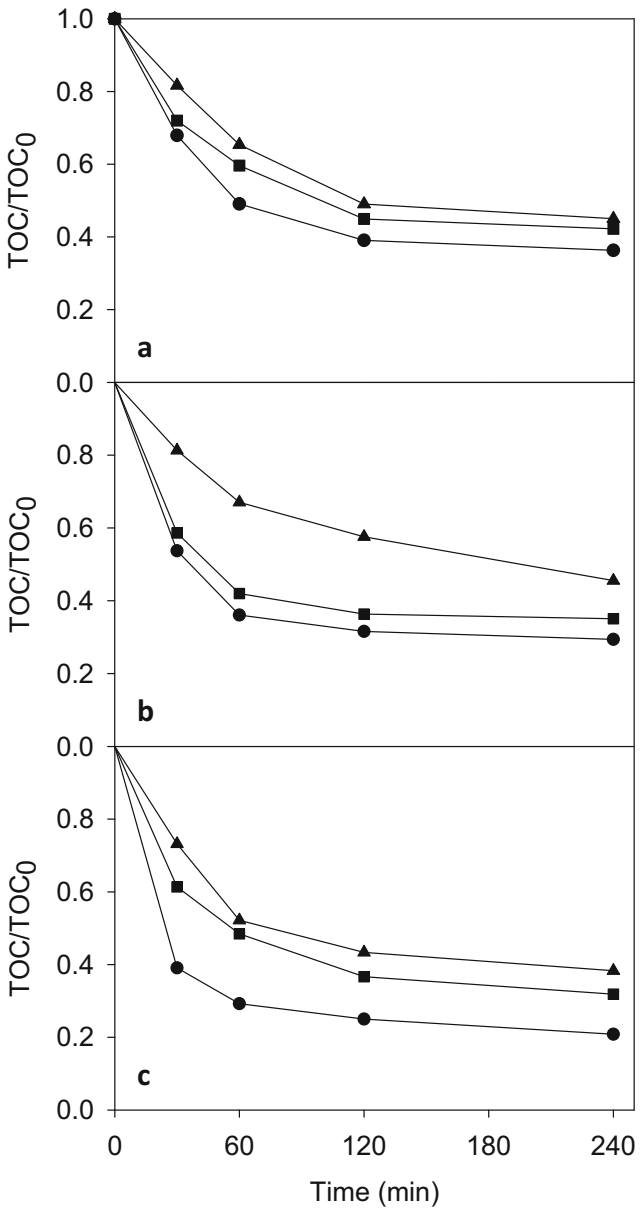

Fig. 3 Effect of the initial Fe^{3+} dosage during the treatment of 1.2 L of 0.1 mM DIA solutions by homogeneous PF process in the presence of **a** 5 mM H_2O_2, **b** 10 mM H_2O_2 and **c** 20 mM H_2O_2, at pH 3, as a function of treatment time. Fe^{3+} dosage, 0.1 mM (*squares*), 0.25 mM (*circles*) and 0.5 mM (*triangles*)

of organic and inorganic supports in order to avoid the generation of iron sludge and to permit the operation in flow system. Initially, experiments were performed using 5.5 g FeS-AB into the bulk. However, the FeS-AB particles were gradually broken during the treatment. These results are in agreement with Barreca et al. (2014), who pointed out the "big fragility" of alginate beads when working with high amounts of H_2O_2 in PF process.

As an alternative matrix, it was decided to use AC as catalyst since it has been described by Karthikeyan and Sekaran

(2014); it promotes the generation of ·OH. According to these authors, the formation of these reactive species takes place by an initial step: the electron transfer (from electron-rich AC) to molecular oxygen to form reactive oxygen species (Eq. 8). Then, the generation of ·OH from the AC($O_2^{\cdot}$) in adsorbed state (AC($O_2^{\cdot}$)$_{ads}$) occurs according to Eq. (9). Additionally, the formation of ·OH could be effectively enhanced by means of the reaction detailed in Eq. (10), promoted by the action of the UV-C light. Accordingly, some authors (Hammouda et al. 2015; Iglesias et al. 2015) already pointed out the efficiency of this material as iron support, without suffering modification of its structure after being reused in the EF treatment.

$$AC(e_{cb}^{-}) + O_2 \rightarrow AC(O_2^{\cdot}) \quad (8)$$

$$AC(O_2^{\cdot})_{ads} + 2H^{+} \rightarrow AC(2\,{}^{\cdot}OH)_{ads} \quad (9)$$

$$AC(h_{vb}^{+}) + h\nu + H_2O \rightarrow AC({}^{\cdot}OH) + H^{+} \quad (10)$$

Based on the aforementioned statements, the use of Fe-AC in PF treatment may improve the generation of ·OH by either the action of activated carbon itself affected by UV-C light or Fenton's reaction between iron immobilized in Fe-AC and H_2O_2 present in the solution.

In order to evaluate the effect of iron concentration, three experiments were performed adding different quantities of Fe-AC into the medium. Thus, 1.25, 3.00 and 6.00 g of Fe-CA were evaluated in the PF experiments using an initial concentration of H_2O_2 of 20 mM. As shown in Fig. 4, the system seems to operate correctly in all cases; however, as in previous experiments, when working at highest iron concentration, i.e. 6.00 g Fe-AC, the process efficiency decreased, thus reducing the final TOC abatement yield of the treatment. On the contrary, the best conditions were found for an intermediate concentration of iron. Thus, after 4 h treatment, 67 % TOC abatement was attained when 3.00 g of Fe-AC and 20 mM of H_2O_2 were added to the solution. Additionally, pH measurements along the treatment confirmed that it kept constant at value around 2.8–3 during 4 h.

The morphology of this catalyst was evaluated by SEM-EDS microscopy (Fig. 5). SEM image (Fig. 5a) and EDS mapping (Fig. 5b) of a Fe-AC ascertained the presence and homogeneous distribution of iron into the AC and reveals that it can be an appropriate support and catalyst in PF process. Moreover, the absence of sludge at the end of the treatment must be highlighted, which constitutes an important advantage in this kind of processes. Therefore, although the obtained results are lower than those achieved by homogenous process, there was no leaching found in the solution at the end of the treatment. Moreover, the high resistance of this matrix (Iglesias et al. 2015) makes possible the reuse of this catalyst or the operation in flow system.

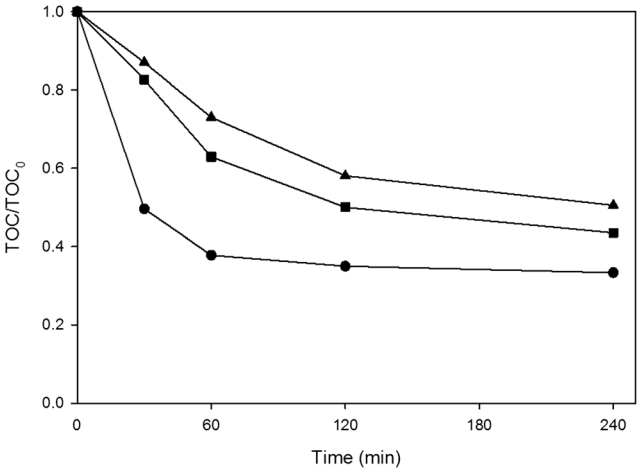

Fig. 4 Effect of the initial Fe-AC dosage after addition of 20 mM H_2O_2 during the treatment of 1.2 L solution of DIA (0.1 mM) by heterogeneous PF process at pH 3 with time, 1.25 g (*squares*), 3 g (*circles*) and 6 g (*triangles*)

Coupling of PF with EF process

After the optimization of the operational parameters involved in the PF process, it was not possible to achieve the complete mineralization of the synthetically polluted solution, thus confirming the formation of very recalcitrant intermediates. This low performance is probably due to wasting reactions (6) and (7) which promoted the presence of excess of H_2O_2 and/or Fe^{2+}. Therefore, these reactions can be avoided by in situ generation of Fenton's reagent, as it occurs in the EF process (Brillas et al. 2009; Oturan and Aaron 2014; Sirés et al. 2014). During this process, H_2O_2 is in situ generated by the two-electron reduction of O_2 (Eq. 11), while the catalyst (Fe^{2+}) is electrochemically regenerated from Fe^{3+} (Eq. 12), promoting the formation of ·OH by Fenton's reaction (Eq. 1). In addition, when the process is performed in an undivided reactor using BDD anode, the formation of physisorbed BDD(·OH) at the electrode surface according to Eq. (13) in addition of the homogeneous ·OH produced in the bulk from Fenton's reaction (Eq. 1), may enhance the elimination of persistent organics (Oturan et al. 2012; Brillas 2014b; Bañuelos et al. 2016; García-Rodríguez et al. 2016).

$$O_{2(g)} + 2H^{+} + 2e^{-} \rightarrow H_2O_2 \quad (11)$$

$$Fe^{3+} + e^{-} \rightarrow Fe^{2+} \quad (12)$$

$$BDD + H_2O \rightarrow BDD({}^{\cdot}OH) + H^{+} + e^{-} \quad (13)$$

Recently, a study has been published by Bocos et al. (2016) reporting the complete mineralization of a 0.1-mM DIA aqueous solution by optimizing the parameters of EF

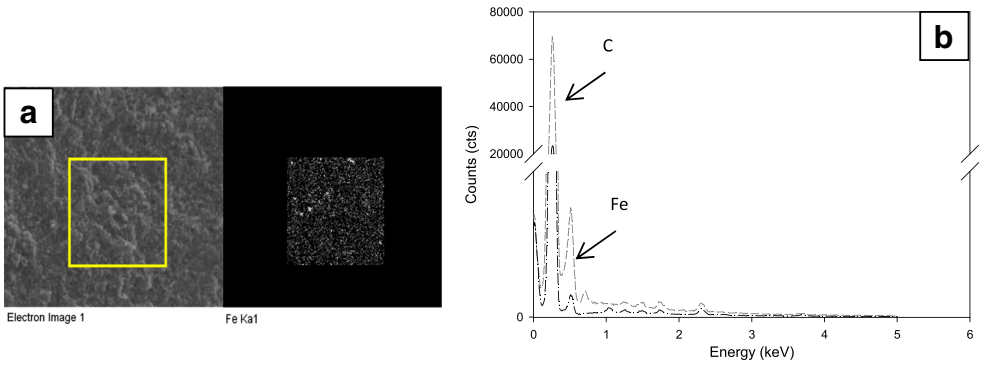

Fig. 5 **a** SEM image and **b** EDS mapping of Fe-AC after adsorption assays

process. They reported that the complete mineralization of DIA solution was reached at a constant current of 1 A. On this context, in order to achieve the total elimination of organic pollutants in this study, two alternatives of coupling between PF and EF processes have been proposed: (i) PF-EF and (ii) conventional PEF.

As observed in Fig. 6, both alternatives allow achieving the total mineralization of organics (DIA and its aromatic/aliphatic intermediates) present in the solution after 120 min of treatment, by applying 22.2 mA/cm^2 of current density. It is remarkable that these results improve those obtained by EF process, where 240 min of treatment time were required to completely mineralize the same concentration of pollutant (Bocos et al. 2016). Nonetheless, the conventional PEF process showed quite higher mineralization efficiency than the sequential PF-EF process. As recently reported by García-Segura et al. (2016), during EF and Fenton process, iron-carboxylate complexes are formed. This species are very recalcitrant and difficult to oxidize due to their low reactivity. However, in most cases, the coupling of PF with EF leads to higher degradation and mineralization abatements in shorter treatment times than the individual process. During PF, $^{\cdot}OH$ are formed by Fenton's reaction (Eq. 1) and at a lesser extent by photolysis of H_2O_2 (Eq. 5) under UV irradiation (Sedaghat et al. 2016) and Fe^{3+} is photo-reduced (Eqs. 2 and 3). In addition, the UV-C light accelerates the decomposition of the iron-carboxylate complexes formed during the treatment, justifying the higher oxidation power of this coupled process (García-Segura et al. 2012; Brillas 2014b). Moreover, by subsequently applying EF treatment, the recalcitrant intermediates formed during PF process can be efficiently oxidized by the (BDD($^{\cdot}OH$) species formed at the anode (Eq. 13) and the $^{\cdot}OH$ generated at the bulk by Fenton's reaction (Eqs. 1 combined to 11 and 12). In addition, there are no accumulation of H_2O_2 and Fe^{2+} in the medium since they are immediately consumed by Fenton's reaction (Eq. 1) thus avoiding the necessity to add high doses of both reagents and consequently minimizing the parasitic reactions (6) and (7). However, the PEF process seems preferable to PF-EF, since better mineralization yield is provided by the former process.

Toxicity assays

Some authors have reported that the formation of by-products is more harmful than the original pollutant during AOPs (Oturan et al. 2008; Dirany et al. 2012). This fact was also described for the treatment of polluted streams by contrast media such as diatrizoate (Real et al. 2009; Gur-Reznik et al. 2011). For this reason, Microtox test was performed to the samples obtained during the treatments and the inhibition ratio was calculated from Eq. (4) for initial samples and after treatment. The initial sample had low toxic effect on the bacteria, showing an inhibition percentage of 14 %. However, after PF treatment, the inhibition percentage was increased until 87.3 %. This fact could be explained by the incomplete mineralization of some photolytic degradation products released in solution which according to Rastogi et al. (2014) could be comparatively more toxic than the parent compound. To identify the toxic products formed during this treatment, GC/MS analysis was carried out and iodoform was detected in treated solution. Iodoform has been reported as a highly cytotoxic and more genotoxic compound in mammalian cells than bromoacetic acid, the most genotoxic of the regulated haloacetics acid (Plewa et al. 2008; Richardson et al. 2008).

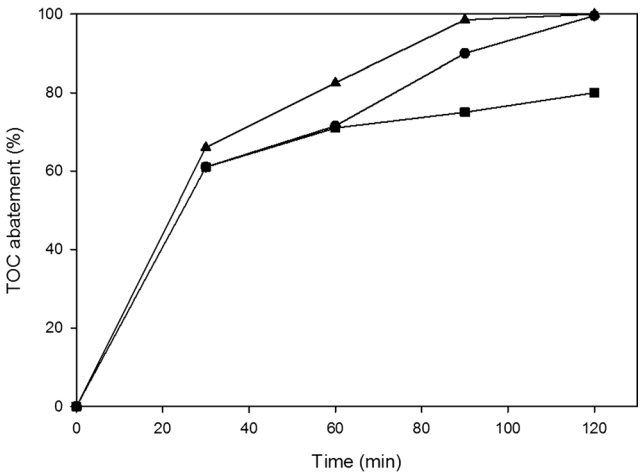

Fig. 6 TOC reduction profile in the different treatments: PF-EF (*circles*), PF (*squares*), and PEF (*triangles*)

On the other hand, the inhibition percentages of PF-EF and PEF treatments were 28 % and 14 %, respectively. Therefore, the proposed treatments favour the total mineralization of the pollutant and the reduction of the toxicity of treated solution.

Conclusion

The mineralization of the contrast agent DIA was carried out under PF treatment. It has been proved the significant influence of the light enhancing the treatment. Besides, different concentrations of H_2O_2 were tested under direct photolysis, demonstrating that concentrations higher than 20 mM end up in detrimental results. Then, homogeneous PF process was carried out in order to find the optimal concentration of Fenton's reagent. Best efficiency was obtained with 20 mM H_2O_2 and 0.25 mM Fe^{3+}. High concentrations of iron (0.5 mM) and H_2O_2 (40 mM) seem to promote parasitic reactions, being prejudicial to the process efficiency. Further, different supports were evaluated for the immobilization of catalyst (Fe^{3+}) to monitor heterogeneous PF process. Fe-AC was found as a suitable alternative that may operate in a continuous process, avoiding the necessity to continuously add this reagent in the medium and preventing the environmental issue related to the formation of the iron sludge at the end of the homogeneous process.

Moreover, the treatment has been successfully enhanced by both proposed alternatives: PF-EF or PEF process, achieving the total mineralization of the solution. Finally, Microtox test demonstrated the positive effect of the application of these complementary treatments on the significant reduction of the solution toxicity.

Acknowledgements This research has been financially supported by the Spanish Ministry of Economy and Competitiveness and ERDF Funds (Projects CTM2014-52471-R). The authors are grateful to the Spanish Ministry of Economy and Competitiveness for the financial support of Elvira Bocos under the FPI programme and the mobility grant: EEBB-I-14-09087.

References

Bañuelos JA, García-Rodríguez O, El-Ghenymy A, Rodríguez-Valadez FJ, Godínez LA, Brillas E (2016) Advanced oxidation treatment of malachite green dye using a low cost carbon-felt air-diffusion cathode. J Environ Chem Eng 4:2066–2075

Barreca S, Colmenares JJV, Pace A, Orecchio S, Pulgarin C (2014) Neutral solar photo-Fenton degradation of 4-nitrophenol on iron-enriched hybrid montmorillonite-alginate beads (Fe-MABs). J Photochem Photobiol A 282:33–40

Bocos E, Pazos M, Sanromán MA (2014) Electro-Fenton decolourization of dyes in batch mode by the use of catalytic activity of iron loaded hydrogels. J Chem Technol Biotechnol 89:1235

Bocos E, Oturan N, Sanromán MÁ, Oturan MA (2016) Elimination of radiocontrast agent diatrizoic acid from water by electrochemical advanced oxidation: kinetics study, mechanism and mineralization pathway. J Electroanal Chem 772:1–8

Bouafia-Chergui S, Oturan N, Khalaf H, Oturan MA (2012) Electrochemical and photochemical oxidation of cationic dyes: a comparative study. Curr Org Chem 16:2073–2082

Bouafia-Chergui S, Oturan N, Khalaf H, Oturan MA (2010) Parametric study on the effect of the ratios $[H_2O_2]/[Fe^{3+}]$ and $[H_2O_2]/[substrate]$ on the photo-Fenton degradation of cationic azo dye basic blue 41. J Environ Sci Health Part A Toxic Hazard Subst Environ Eng 45:622–629

Brillas E, Sirés I, Oturan MA (2009) Electro-Fenton process and related electrochemical technologies based on fenton's reaction chemistry. Chem Rev 109:6570–6631

Brillas E (2014a) A review on the degradation of organic pollutants in waters by UV photoelectro Fenton and solar photoelectro-Fenton. J Braz Chem Soc 25:393–417

Brillas E (2014b) Electro-Fenton, UVA photoelectro-Fenton and solar photoelectro-Fenton treatments of organics in waters using a boron-doped diamond anode: a review. J Mex Chem Soc 58:289–255

Chiou C, Chen Y, Chang C, Chang C, Shie J, Li Y (2006) Photochemical mineralization of di-n-butyl phthalate with H_2O_2/Fe^{3+}. J Hazard Mater 135:344–349

Daud NK, Hameed BH (2010) Fenton-like oxidation of reactive black 5 solution using iron-montmorillonite K10 catalyst. J Hazard Mater 176:1118–1121

Daughton CG, Ternes TA (1999) Pharmaceuticals and personal care products in the environment: agents of subtle change? Environ Health Perspect 107:907–938

Diagne M, Oturan N, Oturan MA, Sirés I (2009) UV-C light-enhanced photo-Fenton oxidation of methyl parathion. Environ Chem Lett 7:261–265

Dias IN, Souza BS, Pereira JHOS, Moreira FC, Dezotti M, Boaventura RAR, Vilar VJP (2014) Enhancement of the photo-Fenton reaction at near neutral pH through the use of ferrioxalate complexes: a case study on trimethoprim and sulfamethoxazole antibiotics removal from aqueous solutions. Chem Eng J 247:302–313

Dirany A, Sirés I, Oturan N, Özcan A, Oturan MA (2012) Electrochemical treatment of the antibiotic sulfachloropyridazine: kinetics, reaction pathways, and toxicity evolution. Environ Sci Technol 46:4074–4082

Fernández de Dios MÁ, Rosales E, Fernández-Fernández M, Pazos M, Sanromán MÁ (2015) Degradation of organic pollutants by heterogeneous electro-Fenton process using Mn-alginate composite. J Chem Technol Biotechnol 90:1439–1447

Florenza X, Solano AMS, Centellas F, Martínez-Huitle CA, Brillas E, Garcia-Segura S (2015) Degradation of the azo dye acid red 1 by anodic oxidation and indirect electrochemical processes based on Fenton's reaction chemistry. Relationship between decolorization, mineralization and products. Electrochim Acta 142:276–288

Florenza X, Garcia-Segura S, Centellas F, Brillas E (2016) Comparative electrochemical degradation of salicylic and aminosalicylic acids: influence of functional groups on decay kinetics and mineralization. Chemosphere 154:171–178

Foo KY, Hameed BH (2009) An overview of landfill leachate treatment via activated carbon adsorption process. J Hazard Mater 171:54–60

García-Rodríguez O, Bañuelos JA, El-Ghenymy A, Godínez LA, Brillas E, Rodríguez-Valadez FJ (2016) Use of a carbon felt–iron oxide air-diffusion cathode for the mineralization of malachite green dye by heterogeneous electro-Fenton and UVA photoelectro-Fenton processes. J Electroanal Chem 767:40–48

Garcia-Segura S, Brillas E (2011) Mineralization of the recalcitrant oxalic and oxamic acids by electrochemical advanced oxidation processes using a boron-doped diamond anode. Water Res 45:2975–2984

Garcia-Segura S, El-Ghenymy A, Centellas F, Rodríguez RM, Arias C, Garrido JA, Cabot PL, Brillas E (2012) Comparative degradation of

the diazo dye direct yellow 4 by electro-Fenton, photoelectro-Fenton and photo-assisted electro-Fenton. J Electroanal Chem 681:36–43
Garcia-Segura S, Brillas E, Cornejo-Ponce L, Salazar R (2016) Effect of the Fe3+/Cu2+ ratio on the removal of the recalcitrant oxalic and oxamic acids by electro-Fenton and solar photoelectro-Fenton, Sol. Energy 124:242–253
Ghaly MY, Härtel G, Mayer R, Haseneder R (2001) Photochemical oxidation of p-chlorophenol by UV/H_2O_2 and photo-Fenton process. A comparative study. Waste Manag 21:41–47
Gur-Reznik S, Azerrad SP, Levinson Y, Heller-Grossman L, Dosoretz CG (2011) Iodinated contrast media oxidation by nonthermal plasma: the role of iodine as a tracer. Water Res 45:5047–5057
Hammouda SB, Adhoum N, Monser L (2015) Synthesis of magnetic alginate beads based on Fe_3O_4 nanoparticles for the removal of 3-methylindole from aqueous solution using Fenton process. J Hazard Mater 294:128–136
Iglesias O, Meijide J, Bocos E, Sanromán MÁ, Pazos M (2015) New approaches on heterogeneous electro-Fenton treatment of winery wastewater. Electrochim Acta 169:134–141
Iglesias O, Gómez J, Pazos M, Sanromán MA (2014) Electro-Fenton oxidation of imidacloprid by Fe alginate gel beads. Appl Catal B Environ 144:416–424
Iglesias O, Fernández de Dios MA, Pazos M, Sanromán MA (2013) Using iron-loaded sepiolite obtained by adsorption as a catalyst in the electro-Fenton oxidation of reactive black 5. Environ Sci Pollut Res 20:5983–5993
Karthikeyan S, Sekaran G (2014) In situ generation of a hydroxyl radical by nanoporous activated carbon derived from rice husk for environmental applications: kinetic and thermodynamic constants. Phys Chem Chem Phys 16:3924–3933
Krzeminska D, Neczaj E, Borowski G (2015) Advanced oxidation processes for food industrial wastewater decontamination. J Ecol Eng 16:61–71
Laurencé C, Rivard M, Thierry M, Morin C, Buisson D, Bourcier S, Sablier M, Oturan MA (2014) Reinvestigation of the oxidative metabolic pathways of furosemide and identification of a toxic metabolite. Chemosphere 113:193–199
Loaiza-Ambuludi S, Panizza M, Oturan N, Oturan MA (2014) Removal of the anti-inflammatory drug ibuprofen from water using homogeneous photocatalysis. Catal Today 224:29–33
Malato S (2008) Removal of emerging contaminants in waste-water treatment: Removal by photo-catalytic processes. Handb Environ Chem Vol 5 Water Pollut 5(S2):177–197
Moreira FC, Garcia-Segura S, Vilar VJP, Boaventura RAR, Brillas E (2013) Decolorization and mineralization of sunset yellow FCF azo dye by anodic oxidation, electro-Fenton, UVA photoelectro-Fenton and solar photoelectro-Fenton processes. Appl Catal B Environ 142-143:877–890
Moreira FC, Garcia-Segura S, Boaventura RAR, Brillas E, Vilar VJP (2014) Degradation of the antibiotic trimethoprim by electrochemical advanced oxidation processes using a carbon-PTFE air-diffusion cathode and a boron-doped diamond or platinum anode. Appl Catal B Environ 160-161:492–505
Murgolo S, Petronella F, Ciannarella R, Comparelli R, Agostiano A, Curri ML, Mascolo G (2015) UV and solar-based photocatalytic degradation of organic pollutants by nano-sized TiO2 grown on carbon nanotubes. Catal Today 240:114–124
Neyens E, Baeyens J (2003) A review of classic Fenton's peroxidation as an advanced oxidation technique. J Hazard Mater 98:33–50
Oh SY, Yoon HS, Jeong TY, Kim SD (2015) Evaluation of remediation processes for explosive-contaminated soils: kinetics and Microtox® bioassay. J Chem Technol Biotechnol 91:928–937
Oturan N, Trajkovska S, Oturan MA, Couderchet M, Aaron JJ (2008) Study of the toxicity of diuron and its metabolites formed in aqueous medium during application of the electrochemical advanced oxidation process "electro-Fenton". Chemosphere 73:1550–1556
Oturan N, Brillas E, Oturan MA (2012) Unprecedented total mineralization of atrazine and cyanuric acid by anodic oxidation and electro-Fenton with a boron-doped diamond anode. Environ Chem Lett 10: 165–170
Oturan MA, Aaron J-J (2014) Advanced oxidation processes in water/wastewater treatment: principles and applications. A review. Crit Rev Environ Sci Technol 44:2577–2641
Papoutsakis S, Afshari Z, Malato S, Pulgarin C (2015) Elimination of the iodinated contrast agent iohexol in water, wastewater and urine matrices by application of photo-Fenton and ultrasound advanced oxidation processes. J Environ Chem Eng 3:2002–2009
Pignatello JJ, Oliveros E, MacKay A (2006) Advanced oxidation processes for organic contaminant destruction based on the Fenton reaction and related chemistry. Crit Rev Environ Sci Technol 36:1–84
Pignatello JJ, Sun Y (1995) Complete oxidation of metolachlor and methyl parathion in water by the photoassisted Fenton reaction. Water Res 29:1837–1844
Plewa MJ, Muellner MG, Richardson SD, Fasano F, Buettner KM, Woo Y, Mckague AB, Wagner ED (2008) Occurrence, synthesis, and mammalian cell cytotoxicity and genotoxicity of haloacetamides: an emerging class of nitrogenous drinking water disinfection byproducts. Environ Sci Technol 42:955–961
Radjenovic J, Flexer V, Donose BC, Sedlak DL, Keller J (2013) Removal of the X-ray contrast media diatrizoate by electrochemical reduction and oxidation. Environ Sci Technol 47:13686–13694
Rastogi T, Leder C, Kümmerer K (2014) Qualitative environmental risk assessment of photolytic transformation products of iodinated X-ray contrast agent diatrizoic acid. Sci Total Environ 482-483:378–388
Real FJ, Javier Benitez F, Acero JL, Sagasti JJP, Casas F (2009) Kinetics of the chemical oxidation of the pharmaceuticals primidone, ketoprofen, and diatrizoate in ultrapure and natural waters. Ind Eng Chem Res 48:3380–3388
Richardson SD, Fasano F, Ellington JJ, Crumley FG, Buettner KM, Evans JJ, Blount BC, Silva LK, Waite TJ, Luther GW, Mckague AB, Miltner RJ, Wagner ED, Plewa MJ (2008) Occurrence and mammalian cell toxicity of iodinated disinfection byproducts in drinking water. Environ Sci Technol 42:8330–8338
Rosales E, Iglesias O, Pazos M, Sanromán MA (2012) Decolourisation of dyes under electro-Fenton process using Fe alginate gel beads. J Hazard Mater 213-214:369–377
Rubio-Clemente A, Chica Arrieta EL, Peñuela Mesa GA (2013) Wastewater treatment processes for the removal of emerging organic pollutants. Rev Ambiente Agua 8:93–103
Rubio-Clemente A, Chica E, Peñuela GA (2015) Petrochemical wastewater treatment by photo-Fenton process. Water Air Soil Pollut 226. doi:10.1007/s11270-015-2321-x
Russo AV, Toriggia LF, Jacobo SE (2014) Natural clinoptilolite-zeolite loaded with iron for aromatic hydrocarbons removal from aqueous solutions. J Mater Sci 49:614–620
Sedaghat M, Vahid B, Aber S, Rasoulifard MH, Khataee A, Daneshvar N (2016) Electrochemical and photo-assisted electrochemical treatment of the pesticide imidacloprid in aqueous solution by the Fenton process: effect of operational parameters. Res Chem Intermed 42:855–868
Sirés I, Brillas E (2012) Remediation of water pollution caused by pharmaceutical residues based on electrochemical separation and degradation technologies: a review. Environ Int 40:212–229
Sirés I, Brillas E, Oturan MA, Rodrigo MA, Panizza M (2014) Electrochemical advanced oxidation processes: today and tomorrow. A review. Environ Sci Pollut Res 8336–8367.
Stüber F, Font J, Fortuny A, Bengoa C, Eftaxias A, Fabregat A (2005) Carbon materials and catalytic wet air oxidation of organic pollutants in wastewater. Top Catal 33:3–50
Stumm-Zollinger E, Fair GM (1965) Biodegradation of steroid hormones. J Water Pollut Control Fed 37:1506–1510

Ternes TA, Stüber J, Herrmann N, McDowell D, Ried A, Kampmann M, Teiser B (2003) Ozonation: a tool for removal of pharmaceuticals, contrast media and musk fragrances from wastewater? Water Res 37:1976–1982

Tiehm A, Schmidt N, Stieber M, Sacher F, Wolf L, Hoetzl H (2011) Biodegradation of Phmaceutical compounds and their occurrence in the Jordan Valley. Water Resour Manag 25:1195–1203

Umar M, Aziz HA, Yusoff MS (2010) Trends in the use of Fenton, electro-Fenton and photo-Fenton for the treatment of landfill leachate. Waste Manag 30:2113–2121

Velo-Gala I, López-Peñalver JJ, Sánchez-Polo M, Rivera-Utrilla J (2012) Ionic X-ray contrast media degradation in aqueous solution induced by gamma radiation. Chem Eng J 195–196:369–376

Velo-Gala I, López-Peñalver JJ, Sánchez-Polo M, Rivera-Utrilla J (2014) Comparative study of oxidative degradation of sodium diatrizoate in aqueous solution by H_2O_2/Fe^{2+}, H_2O_2/Fe^{3+}, Fe (VI) and UV, H_2O_2/UV, $K_2S_2O_8$/UV. Chem Eng J 241:504–512

Xu P, Han H, Zhuang H, Hou B, Jia S, Xu C, Wang D (2015) Advanced treatment of biologically pretreated coal gasification wastewater by a novel integration of heterogeneous Fenton oxidation and biological process. Bioresour Technol 182:389–392

Zhao C, Arroyo-Mora LE, DeCaprio AP, Sharma VK, Dionysiou DD, O'Shea KE (2014) Reductive and oxidative degradation of iopamidol, iodinated X-ray contrast media, by Fe(III)-oxalate under UV and visible light treatment. Water Res 67:144–153